Research Article

Journal of Environmental Nanotechnology

Nano-Titanium Dioxide: Antioxidant Activity and Cytotoxicity Against Human Lung Cancer Cell Line

Blessymol B[1], V. Kalaiselvi[1*], P. Yasotha[1], S. Gopi[2] and S. Ramanathan[2]

[1]Department of Physics, Navarasam Arts and Science College for Women, Arachalur, Erode, TN, India
[2]Department of Physics, Sri Ramakrishna Mission Vidyalaya College of Arts and Science, Coimbatore, TN, India
Received: 25.03.2024 Accepted: 29.03.2024 Published: 30.03.2024
*nk.arthi.kalai@gmail.com

ABSTRACT

The scope of this study is to synthesize titanium dioxide nanoparticles by chemical method and to assess their antioxidant and anticancer properties. Titanium isopropoxide was employed as a precursor in the production of the nanoparticles of titanium dioxide. The sample was analyzed using a variety of characterization techniques, including X-ray diffraction, Ultraviolet-Visible Spectroscopy, Fourier Transform Infrared Spectroscopy, Field Emission Scanning Electron Microscopy, Energy Dispersive X-ray analysis. Further, their antioxidant and anticancer activities have been investigated. The crystallite size of titanium dioxide nanoparticles was revealed by X-ray diffraction, and the functional groups were confirmed by Fourier Transform Infrared Spectroscopy. Field emission scanning electron microscopy and energy dispersive X-ray analysis reveal the structure of the nanoparticles and the presence of titanium, carbon, and oxygen molecules, respectively. The antioxidant activity indicates that as the concentration of the TiO_2 nanoparticles increases, it reaches the activity of ascorbic acid (standard). The sample shows good cytotoxic effect against A549 human lung cancer cell lines.

Keywords: TiO_2; Antioxidant; Fourier Transform Infrared Spectroscopy; Energy dispersive X-ray analysis; Anticancer activity.

1. INTRODUCTION

Cancer, a form of tumor, is the uncontrolled growth of cells in an organ or any part of the body that continues to spread over time. This fatal disease claims nearly 10 million lives every day. Root causes of cancer are unpredictable but health professionals proclaim that if cancer is persistent in one generation or more, it can be deemed as a hereditary disease. Titanium dioxide commonly known as (TiO_2) is a white, poorly soluble substance that finds extensive applications in the biomedical fields (Jafari *et al.* 2020). Certain characteristics of titanium dioxide include resistance to chemical erosion, non-toxicity, antibacterial, antioxidant, and anticancer effects (Blessymol *et al.* 2023).

Titanium dioxide nanoparticles also have unique features that set them apart from other types of nanoparticles produced *via* chemical or environmentally friendly approaches. Due to their exceptional optical and electrical properties, chemical stability, and environmental friendliness, titanium dioxide nanoparticles are the most often employed materials in various applications (Seman *et al.* 2022). Titanium dioxide nanoparticles are employed in cell line investigations. This produces reactive oxygen species (ROS), which split DNA and cause necrosis and apoptosis. The impact of nanoparticles has been examined using A549 cell line, a human adenoma lung cancer cell line (Hariharan *et al.* 2020).

The goal of the current study is to synthesize titanium dioxide nanoparticles by sol gel method. The structural, morphological, vibrational, and optical characteristics of chemically produced titanium dioxide nanoparticles were investigated. Additionally, the antioxidant and anticancer activities were evaluated.

2. MATERIALS AND METHODS

2.1 Materials Used

Analytical reagent grade (99%) titanium tetra isopropoxide was purchased from Sigma Aldrich.

2.2 Synthesis of TiO_2 Nanoparticles

The procedure for synthesizing TiO_2 nanoparticles was adopted from a literature method (Punitha *et al.* 2020). About 5 mL of titanium tetra isopropoxide was added to 30 mL of distilled water taken in a beaker. The mixture was stirred for 30 minutes using a magnetic stirrer. Formation of a white solution indicated the conversion of the precursor into TiO_2. The solution was kept at microwave oven at 70 °C. A white colour powder was obtained after the solvent evaporated. The powder was calcinated at 200 °C in muffle furnace for half an hour to obtain white colour TiO_2 nanopowder. Furthermore, the prepared white powder was ground subtly using a mortar and pestle to get fine TiO_2 nanopowder (denoted as PT).

Chemical Reaction:

$$Ti(OCH(CH_3)_2)_4 + 2H_2O \rightarrow TiO_2 + 4(CH_3)_2CHO$$

2.3 Characterization Techniques

2.3.1 FTIR Analysis

The vibrational frequencies of bonds in the synthesized TiO_2 nanoparticles have been identified using FTIR analysis. The spectrum was recorded on a Perkin-Elmer 100 spectrophotometer in the range 4000–400 cm^{-1}.

2.3.2 UV Visible Spectroscopy

The optical features of the sample are determined using UV-visible spectroscopy. The absorbance was measured in the wavelength region 200–800 nm using a Shimadzu UV 2450 UV-Visible Spectra photometer (Anitha *et al*. 2022).

2.3.3 Field Emission Scanning Microscope

The morphology of the produced sample was examined with an FEI-QUANTA-FEG 250 Field Emission Scanning Microscope.

2.3.4 EDAX Analysis

EDAX (6490 LA) was used to record the chemical composition of the samples at a 20 kV acceleration voltage. EDAX analysis predicts the presence of elements in the prepared sample.

2.3.5 X-ray Diffraction

An investigation of powder X-ray diffraction was conducted on an XPERT-PRO instrument with CuKα radiation (Nancy *et al*. 2022). The microstrain, dislocation, lattice parameters, unit cell volume and atomic packing factor were also calculated by XRD pattern.

2.3.6 Evaluation of *in vitro* Antioxidant Activity of Titanium dioxide (TiO_2) Nanoparticles

Antioxidant activity of the metal nanoparticles was determined by 2,2-diphenyl-1-picrylhydrazyl (DPPH) free radical scavenging assay. The free radical scavenging ability of PT against DPPH radicals was determined by the decrease in absorbance induced by the sample. The DPPH solution with a concentration of 0.1 mM was prepared in 100 mL methanol. Methanolic DPPH solution (100 µL) is added to 300 µL of the solution of the sample (PT) at different concentrations (500, 250, 100, 50 and 10 µg/mL). The mixtures were shaken and allowed to stand at room temperature for 30 minutes. The absorbance of the resultant solution was measured at 517 nm and ascorbic acid was used as the reference. The DPPH solution without sample or standard was used as the blank. The radical scavenging activity was calculated using equation (1).

$$\text{DPPH Scavenging Effect (\% inhibition)} = \frac{\text{absorbance of control} - \text{absorbance of reaction mixture}}{\text{absorbance of control}} \times 100 \quad \ldots (1)$$

2.3.7 Cell Viability Assay

The cell line A549 (Lung Carcinoma) was purchased from National Centre for Cell Science (NCCS) Pune, India. The assays for cytotoxicity were conducted on 96-well plates. Cells were seeded into each well of the 96-well plates, and then the cells were incubated in a CO_2-filled incubator with 5% CO_2 and a 95% humidity atmosphere. A volume of 50 µL of the culture was incubated with 100 µL of 2-(4, 4-dimethyl-2-tetrazoyl)-2, 5-diphenyl-2, 4-tetrazolium salt (MTT) at 37 ℃ for three hours. Following the incubation period, 200 µL of phosphate-buffered saline was added to each sample, and excess MTT was carefully drained off. For solubilization, 200 µL of acid-propanol was added and kept in the dark overnight. Using a microtitre plate reader, the absorbance was measured at 650 nm. The percentage vitality of the cells in the other treatment groups was computed using equation (2), and the optical density of the control cells was fixed to be 100% viable.

$$\text{\% Viability} = \frac{\text{Control OD} - \text{Sample OD}}{\text{Control OD}} \times 100 \quad \ldots (2)$$

3. RESULTS AND DISCUSSION

3.1 Functional Group Analysis

The presence of different functional groups is revealed by FTIR Analysis. The IR spectrum of TiO_2 is shown in Fig. 1. The peaks at 331cm^{-1} and 1643 cm^{-1} reveal the surface water or hydroxyl groups (Manal *et al*. 2022) and carbonyl groups in the prepared sample (Annin *et al*. 2022). The carbonyl stretching vibration was found at 2112 cm^{-1} (B. Blessymol *et al*. 2023). The peak at 1136 cm^{-1} is ascribed to the C-O bond stretches in the sample. The peak at 690 cm^{-1} corresponds to O-Ti-O bonding (Srujana *et al*. 2022). The stretching mode of Ti-O-Ti is observed at 420 cm^{-1} (Annin *et al* 2022; Harpreet *et al*. 2019).

3.2 UV Analysis

The UV-Visible absorption spectrum and Tauc's plot for the prepared sample are shown in Fig. 2. An absorption peak was observed at 258 nm. Hong *et al.* (2013) have found the absorption peak of bulk TiO_2 at 263 nm, which is greater than that of the TiO_2 nanoparticles.

The numerical derivative of the optical absorption coefficient was employed for estimating the

band gap energy. Band-to-band transitions are examined using the energy relation in the basic absorption approach. E=hν, where h is the Planck's constant, ν=c/λ, where c is the speed of the light in vacuum and λ is the wavelength of the spectrum (Vetrivel *et al*. 2015). The shift of electrons from the valence band to the conduction band may cause the absorbance to drop after 258 nm (Manikandan *et al*. 2017).

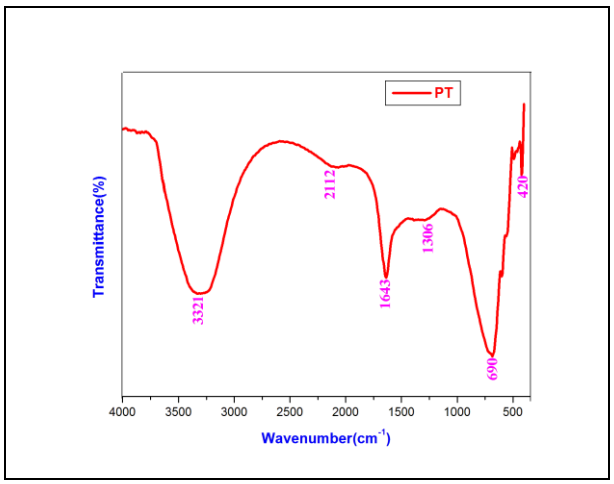

Fig. 1: FTIR spectrum of the prepared TiO_2 nanoparticles

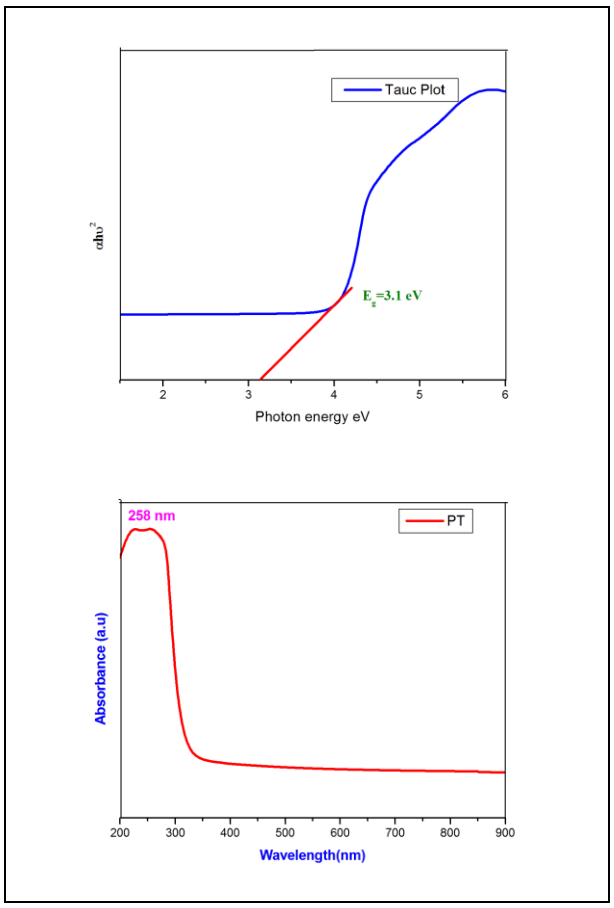

Fig. 2: UV-Visible absorption and Tauc's plot of the prepared sample

The band gap energy (E_g) is also calculated by this absorption peak using well known Tauc's equation (equation 3).

$$(\alpha h\nu)=A(h\nu-E_g)^n \quad \ldots. (3)$$

where α is an absorption coefficient, h is the Planck's constant (6.626×10^{-34} joules sec), ν is the light frequency, A is the constant, E_g is the optical band gap of TiO_2 and n is the constant which depends on the characteristics of the transition bands. The E_g value is 3.1 eV which matches with that of the bulk TiO_2 (3.2 eV) (Arvind *et al*. 2021).

3.3 Field Emission Scanning Electron Microscopy Analysis

The shape and average grain size of the prepared sample were determined using FESEM analysis. The FESEM images demonstrated the spherical shape of TiO_2 (Yamkela *et al*. 2023). The measured average particle size for pure TiO_2 is 104.1 nm (Fig. 3). Furthermore, the magnified images of TiO_2 nanoparticles are illustrated in the same figure. The FESEM image at 200 nm shows spherical shape whereas at 2 µm, the image was agglomerated.

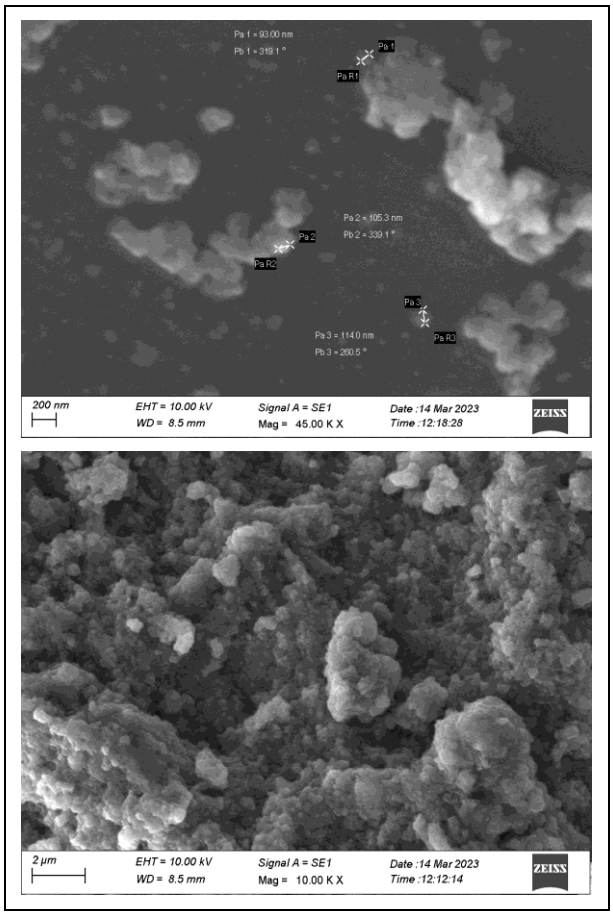

Fig. 3: FESEM image of the prepared sample

3.4 Energy Dispersive X-ray Analysis

The chemical composition of the prepared sample was confirmed through EDAX spectra. The EDAX spectrum of the prepared TiO_2 nanoparticles is illustrated in Fig. 4. The elements Ti, O, C and other trace elements are present in the synthesized nanomaterial. The composition of titanium element is much higher compared with other elements. This shows that no additional impurities have been formed in the preparation.

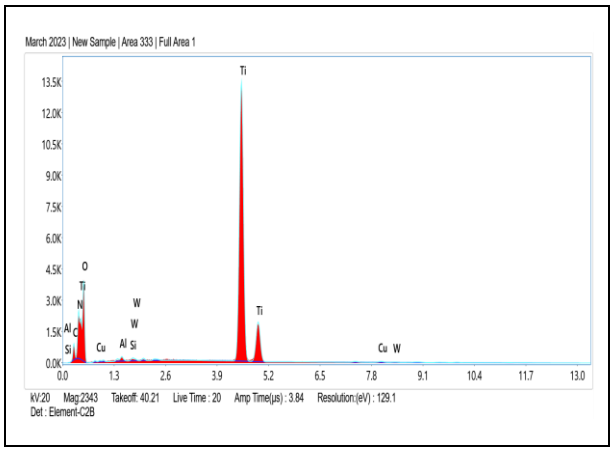

Fig. 4: EDAX spectra of TiO_2 Nanoparticles

Table 1: Atomic and weight percentage of the TiO_2 Nanoparticles

Element	Weight %	Atomic %
C K	4.59	9.28
N K	2.09	3.62
O K	39.42	59.86
Al K	0.41	0.37
Si K	0.08	0.07
Ti K	52.23	26.50
Cu K	0.59	0.22
W L	0.60	0.08

The atomic and weight percentages of the TiO_2 nanoparticles are collected in Table 1. The equipment used to prepare the sample possesses elements like Si, Al, W, and so they show peaks in the spectrum.

3.5 X-ray Diffraction Analysis

X-ray analysis was used to determine the structural characteristics of the produced TiO_2 nanoparticles (PT) (Vella *et al*. 2021). The nanoscale range of the produced material is demonstrated by the line broadening of the diffraction peak. The XRD pattern of the prepared sample in orthorhombic phase is shown in Fig. 5. The peaks at 25°, 31° , 38°, 48°,54°, 63°, 69° and 75° correspond to (2 1 0), (0 2 0), (4 0 0), (0 2 2), (1 3 1), (1 3 2), (0 4 0) and (5 3 1) h k l planes matched with JCPDS Card No:76-1934. No other impurity peaks were formed. The crystallite size and peak broadening profile of the synthesized nanoparticles were estimated by Debye Scherrer formula ($D=0.9\lambda/\beta \cos\theta$), where β is the full width half maximum of the diffraction peak, θ indicates the Bragg's diffraction angle, λ is equal to 0.15409 nm (wavelength of the X-ray) and D denotes the average crystallite size in nm. Similarly, microstrain and dislocation density, lattice parameters, unit cell volume and atomic packing fraction were also calculated as per formula and shown in Table 2.

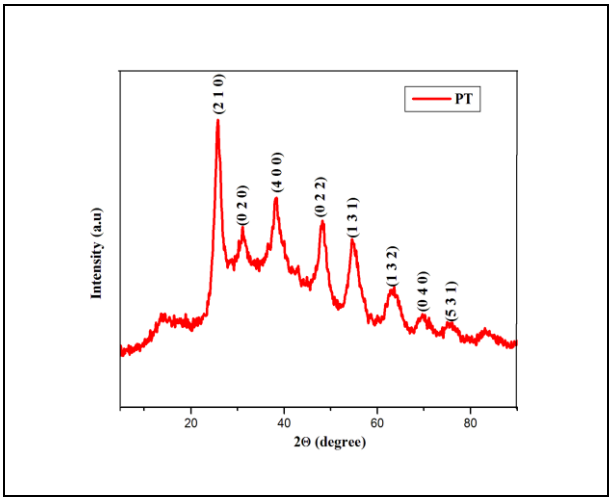

Fig. 5: XRD pattern of TiO_2 Nanoparticles

Table 2. Structural parameters for the prepared sample

Sample Name	Avg. Crystallite size $D = \frac{0.9\lambda}{\beta cos\theta}$ (10^{-9}) m	Microstrain $\varepsilon = \frac{\beta \cos\theta}{4}$ (10^{-3}) m	Dislocation $\delta = \frac{1}{D^2}$ (10^{15}) lines/ m^2	Lattice Parameters Å	Unit cell V = abc $(Å)^3$	Atomic Packing factor $APF = \frac{\frac{4}{3}\pi r^3}{3abc}$ where $r = \frac{\sqrt{3}}{4}a$
PT	71.92	5.402	0.19	a=2.14 b=5.75 c= 5.00	61.418	0. 054

The average crystallite size for the prepared sample was calculated as 71.92 nm. The crystallinity of the sample gets enhanced. For orthorhombic structure, the lattice constant can be estimated from the formula

$$\frac{1}{d^2} = \frac{h^2}{a^2} + \frac{k^2}{b} + \frac{l^2}{c^2}$$

For (2 1 0), (0 2 0), the d values were calculated as 3.43990, 2.87070, respectively. The lattice parameters a=2.14, b=5.75 and c= 5.00 values are good and match with the standard values in JCPDS Card No: 76-1934. The calculated microstrain and dislocation values are 5.402 $\times 10^{-3}$ m and 0.19 $\times 10^{15}$ lines/ m^2.

3.6 Photoluminescence Analysis

The photoluminescence (PL) spectra of the pure TiO_2 is shown in Fig. 6. The absorbance was taken at 275 nm. It shows strongest emission peak at 351 nm. The PL emission may results from recombination of excited electron hole pairs and low emission intensity indicates the low intensity of recombination rate. The luminescence efficiency depends on the absorption emission of TiO_2 nanoparticles at 351 nm. In the excited state, it can produce a little non-radioactive transition.

3.7 Antioxidant Activity

The antioxidant activity of the prepared titanium dioxide nanoparticles was performed using the DPPH assay method. The results are presented in Fig. 7 and Table 3. The compound DPPH has a noticeable absorption band and a rich purple color. The decrease in DPPH indicates the ability of nanoparticles to scavenge these radicals. The DPPH solution initially has a deep violet color, but when the reactivity of the test sample increases, it loses its purple color. This proves the capability of nanoparticles to scavenge them. These findings demonstrate that the scavenging activity of the nanoparticles increased as their concentration increased (Imran *et al*. 2018).

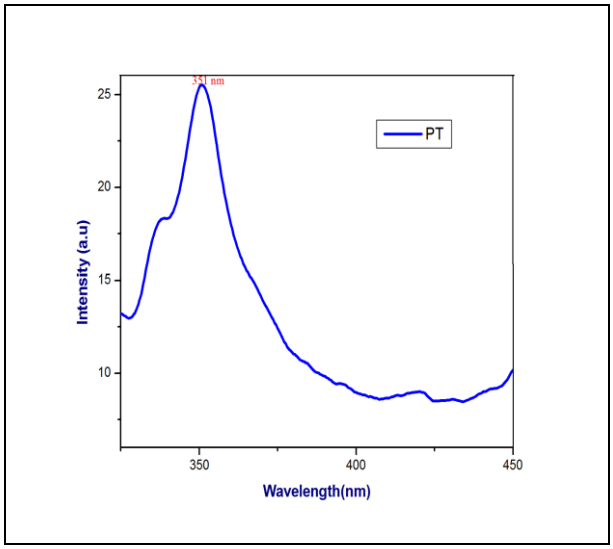

Fig. 6: PL spectra of the TiO_2 Nanoparticles

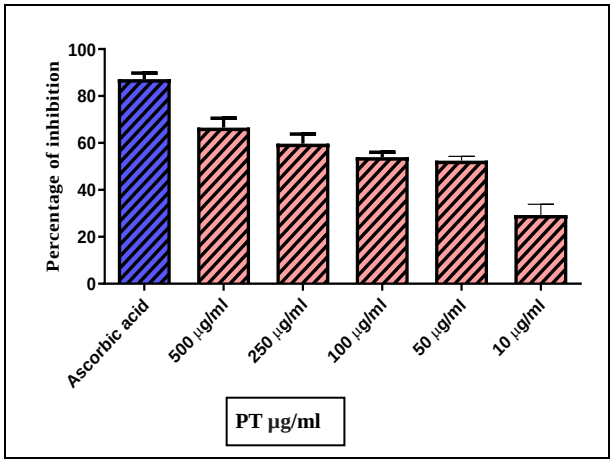

Fig. 7: Scavenging activity of the prepared sample

Table 3. Percentage inhibition of the prepared sample

S. No.	Tested sample concentration (µg/mL)	Percentage of inhibition (in triplicates)			Mean value (%)
1.	Ascorbic acid	90.08674	86.36927	85.13011	87.19537
2.	500	64.06444	64.31227	71.12763	66.50145
3.	250	64.43618	57.00124	57.62082	59.68608
4.	100	55.51425	51.67286	54.77076	53.98596
5.	50	52.7881	54.15118	50.55762	52.49897
6.	10	24.16357	32.83767	30.97893	29.32672

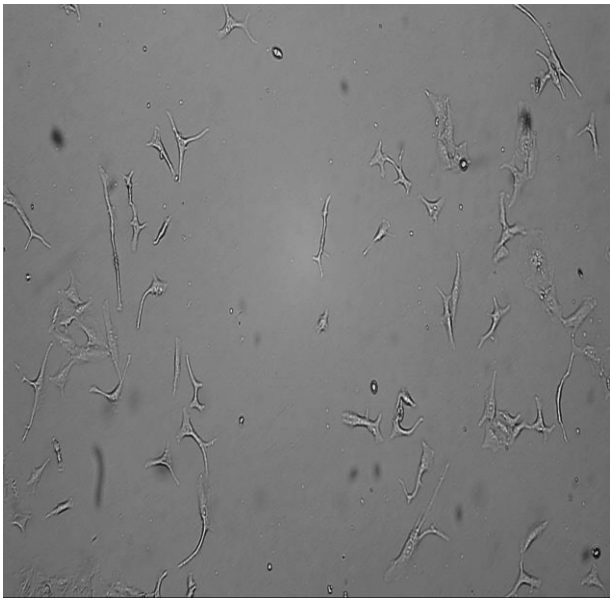

Fig. 8: Etoposide treated cells

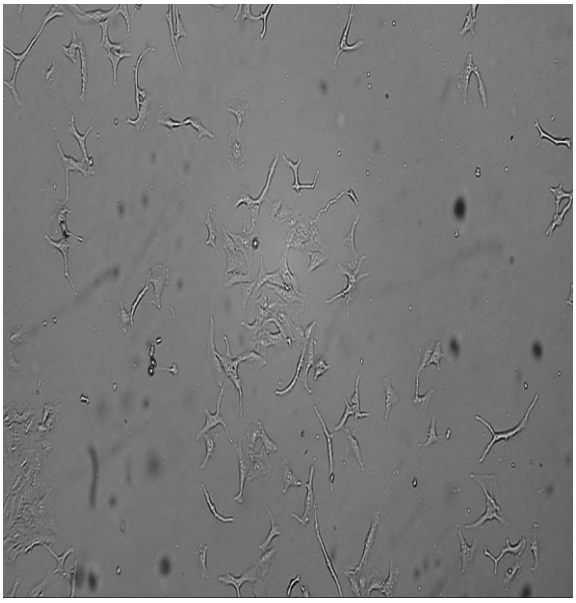

Fig. 9: Anticancer activity of the prepared sample

3.8 Anticancer Activity

Cell viability assay of the prepared sample was studied using A549 cell lines (Hariharan *et al*. 2017). The primary function of anticancer drugs is to decrease anticancer apoptosis. The most widely used basic cytotoxic assay to estimate anticancer activity is the MTT assay. In the current study, TiO2 nanoparticles were treated against A549 cell lines. The percentage of cytotoxicity increases as the concentration of the sample increases gradually. The Etoposide treated cells and Anticancer activity of the prepare sample is illustrated in the Figure 8 and 9. The % of cytotoxicity for 125µg prepared sample was 63.57, which indicates that our sample will fight the cancer cells at the initial stage. The graph against % of inhibition and concentration µg/ml is illustrated in the Figure 10. The results showed that the prepared samples transmit cytotoxic effect with regard to the A549 cell lines within 24 hours of treatment. This proves that the prepared samples possess effective cytotoxic effect against the A549 cell lines and further tested for in vivo trials.

Cell viability assay of the prepared sample was studied using A549 cell lines (Hariharan *et al*. 2017). The primary function of anticancer drugs is to decrease anticancer apoptosis. The most widely used basic cytotoxic assay to estimate anticancer activity is the MTT assay. In the current study, TiO_2 nanoparticles were tested against A549 cell lines for their cytotoxicity (Fig. 9). The percentage of cytotoxicity increases as the concentration of the sample increases gradually. The % of cytotoxicity for 125 µg prepared sample was 63.57, which indicates the sample will fight the cancer cells at the initial stage. The graph against % of inhibition and concentration µg/mL is illustrated in Fig.10. The results showed that TiO_2 nanoparticles exhibit cytotoxic effect with regard to the A549 cell lines within 24 hours of treatment. This suggests that the compound can be subjected to *in vivo* trials.

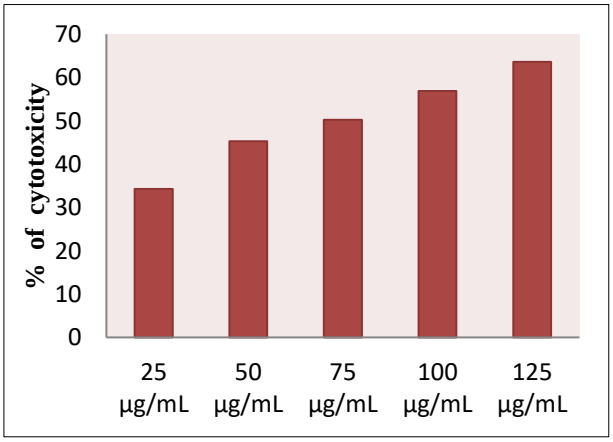

Fig. 10: Anticancer activity of the prepared sample

4. CONCLUSION

The current effort aimed to produce titanium dioxide nanoparticles by a simple method. The orthorhombic structure of the prepared nanoparticles was revealed by the XRD analysis. FTIR spectroscopy was used to confirm the existence of the Ti-O bond. The carbon, and oxygen in the produced nanoparticles, while the FESEM picture reveals the spherical shape of the particles. Using UV-visible spectrophotometer, the

adsorption peak was identified, and the DPPH assay served to evaluate the antioxidant capacity. The cytotoxicity of the nanoparticles against A549 cell lines assessed by MTT assay shows encouraging results.

REFERENCES

Anith, J. R., Devina, M. D., Arulananth, T. S. and Nagaraju, S., Characterization Analysis of Silver Nanoparticles Synthesized from Chaetoceros calcitrans, *J. Nanomater*., 2022, 1-15 (2022). https://doi.org/10.1155/2022/4056551

Annin, K. S., Hiwa, M. A., Muhammad, W., Snehlata, K., Saikh, M. W., Gaber, E. E., Md, A. I. and Kantilal, P. R., Synthesis and applications of green synthesized TiO_2 nanoparticles for photocatalytic dye degradation and antibacterial activity, *J. Nanomater*., 2022, 1-9 (2022). https://doi.org/10.1155/2022/7060388

Annin, K. S., Saikh, M. W., Masoom, R. S., Md, A. I., Kantilal, P. R. and Arul, J. T. S., Photocatalytic activity of green construction TiO_2 nanoparticles from Phyllanthus niruri leaf extract, *J. Nanomater*., 2022, 1-11 (2022). https://doi.org/10.1155/2022/7011539

Archana, A., Chaudhari, Umesh, J. T., Arun, V. P., Chandrakant, G. D., Synthesis And Characterization Of Zinc Oxide Nanoparticles Using Green Synthesis Method, *Int. J. Creative Res. Thoughts*, 10(2), 302-309 (2022).

Arvind, M., Amalanathan, M. and Sony, M. M. M., Synthesis of TiO_2 nanoparticles by chemical and green synthesis methods and their multifaceted properties, *SN Appl. Sci.*, 3, 409 (2021). https://doi.org/10.1007/s42452-021-04281-5

Blessymol, B., Kalaiselvi, V., Yasotha, P. and Gopi, S., Comparative study of chemically and green synthesized Titanium dioxide nanoparticles using Leucas aspera leaf extract, *J. Environ. Nanotechnol.*, 12(3), 10-13 (2023). https://doi.org/10.13074/jent.2023.09.233471

Hariharan, D., Srinivasan, K. and Nehru, L. C., Synthesis and characterization of TiO_2 nanoparticles using cynodon dactylon leaf extract for antibacterial and anticancer (a549 cell lines activity), *J. Nanomater. Res.*, 5(6), 1-12 (2017). https://doi.org/10.15406/jnmr.2017.05.00138

Hariharan, D., Thangamuniyandi, P., Jegatha, Christy, A., Vasantharaja, R., Selvakumar, P., Sagad evan, S., Pugazhendhi, A., Nehru, L. C., Enhanced photocatalysis and anticancer activity of green hydrothermal synthesized Ag@TiO_2 nanoparticles, *J. Photochem. Photobiol., B*, 202, 111636 (2020). https://doi.org/10.1016/j.jphotobiol.2019.111636

Harpreet, K., Simerjeet, K., Jagpreett, S., Mohit, R. and Sanjeev, K., Expanding horizon:green synthesis of TiO_2 nanoparticles uaing Carica papaya leaves for photocatalysis application, *Mater. Res. Express*, 6(9), 095034 (2019). https://doi.org/10.1088/2053-1591/ab2ec5

Hong, S. M., Lee, S. and Jung, H. J., Simple preparation of anatase Tio2 nanoparticles via pulsed laser ablation in liquid, *Bulletin of Korean Chemistry Society*, 34(1), 279–282 (2013). https://doi.org/10.5012/bkcs.2013.34.1.279

Imran, A., Mohd, S., Zied, Alothman, A. and Abdulrahman, A., Recent advances in syntheses, properties and applications of TiO_2 nanostructures, *RSC Advances*, 53(8), 30125-30147 (2018). https://doi.org/10.1039/C8RA06517A

Jafari, S., Mahyad, B., Hashemzadeh, H., Janfaza, S., Gholikhani, T. and Tayebi, L., Biomedical Applications of TiO_2 Nanostructures: Recent Advances, *Int. J. Nanomedicine*, 2020(12), 3447-3470 (2020). https://doi.org/10.2147/ijn.s249441

Manal, A. A., Meznah, M. A., Awatif, A. H., Promy, V., Albandari, W. A., Taghreed, B., Fatehia, S. A., Fatma, A. and Eiman, M. I., Potential role of green synthesized Titanium Dioxide nanoparticles in photocatalytic applications, *Cryst.*, 12(11), 1-10 (2022). https://doi.org/10.3390/cryst12111639

Manikandan, K., Jafar, A. A. and Brahmanandhan, G. M.m Synthesis, Structural and Optical Characterization of TiO2 Nanoparticles and its Assessment to Cytotoxicity Activity, *J. Environ. Nanotechnol.*, 6(3), 94-102 (2017). https://doi.org/10.13074/jent.2017.09.173273

Nancy, J., Kalaiselvi, V., Blessymol, B., Yasotha, P., Vishalatchi, M. and Pavithra, S., Microwave Synthesis of Triethanolamine-doped Zinc Oxide Nanoparticles, *J. Environ. Nanotechnol.*, 11(2), 22-27 (2022) https://dx.doi.org/10.13074/jent.2022.06.222454

Punitha, V. N., Vijayakumar, S., Sakthivel, B. and Praseetha, P. K., Protection of neuronal cell lines, antimicrobial and photocatalytic behaviours of eco-friendly TiO_2 nanoparticles, *J. Environ. Chem. Eng.*, 8(5), 104343 (2020). https://doi.org/10.1016/j.jece.2020.104343

Seman, N., Tarmizi, Z. I., Ali, R., Taib, S. H. M., Salleh, M. S. N., Zhe, J. C. and Mohamad S. S. N. A., Preparation Method of Titanium Dioxide Nanoparticles and Its Application: An Update, *IOP Conf. Ser.: Earth Environ. Sci.*, 1091, 012064 (2022). https://doi.org/10.1088/1755-1315/1091/1/012064

Srujana, S., Anjamma, M., Alimuddin, Bharat, S., Ram, C. D., Shanthi, N. and Ramana, H., A comprehensive study on the synthesis and characterization of TiO_2 nanoparticles using aloe vera plant extract and their photocatalytic activity against MB dye, *Adsorpt. Sci. Technol.*, 2022, 1-9 (2022). https://doi.org/10.1155/2022/7244006

Vella, D. S. C., Kumar, E. and Muthuraj, D., Investigations on structural, optical, and impedance Spectroscopy studies of titanium dioxide nanoparticles, *Bull. Chem. Soc. Ethiop*., 35(1), 151-160 (2021). https://dx.doi.org/10.4314/bcse.v35i1.13

Vetrivel, V., Rajendran, K. and Kalaiselvi, V., Synthesis and characterization of pure titanium dioxide nanoparticles by sol-gel method, *Int. J. Chem Tech Res.*, 7(3), 1090-1097 (2015).

Yamkela, M., Jerry, O. A., Doctor, M. N. M., Moganavelli, S., Damian, C. O., Green synthesis, antioxidant and anticancer activities of TiO2 nanoparticles using aqueous extract of Tulbhagia violacea, *Results Chem.*, 6, 101007 (2023). https://doi.org/ 10.1016/j.rechem.2023.101007